THE BELL SYSTEM TECHNICAL JOURNAL
Vol. 51, No. 9, November, 1972
Printed in U.S.A.

Waveguide Breakdown Effects at High Average Power and Long Pulse Length

By A. S. ACAMPORA and P. T. SPROUL

(Manuscript received March 17, 1972)

Analytical predictions of the power handling capabilities of waveguide systems generally have not considered the effects of high average power and long pulse length. It has experimentally been noted, however, that a substantial reduction in power handling capability below expected levels does occur as average power and pulse length are increased. This reduction can be attributed to the presence of loose particulate matter which is heated by the average power, causing localized rarefication of the dielectric gas fill as well as the expected voltage enhancement.

An unstable arcing situation is shown to exist when the arc duration exceeds some critical time. Typical pulse lengths in use today exceed this critical time and may result in continuous arcing. The use of control circuitry to terminate each particle-induced arc prevents continuous arcing and deletes the particle, and is therefore essential to stable operation at long pulse lengths and high average power.

I. INTRODUCTION

An understanding of microwave breakdown in gases has existed for many years[1,2] and has been successfully applied to the design of many high-power microwave systems operating at low duty cycles with pulse lengths on the order of several microseconds. However, recent testing of S-band WR284 microwave hardware filled with sulfur hexafluoride (SF_6) and operated at 500- to 1500-kilowatt average power, and 10- to 150-megawatt peak power with 50- to 150-microsecond rectangular pulses showed performance far below expectation. A series of tests and supporting analytical work were undertaken to explain this behavior. These have shown that the empirically observed reduction in peak power handling capability at high levels of average power is caused by the presence of loose particulate matter, microscopic in size and lossy at microwave frequencies. The experimental and analytical proof of the mechanisms responsible for this effect is described. A procedure is

presented employing short duration discharges to break up these particles, thereby increasing power handling capability.

Waveguide cavities and resonant ring structures of various lengths were tested because the empirical peak breakdown power level was found to decrease with resonator length. It is shown that this effect is related to the arc energy absorption which is dependent upon resonator length. A quantitative understanding of this phenomenon is developed and is applied to confirm the experimental results.

II. BREAKDOWN MECHANISMS

The parameters which affect the peak power handling capability of a microwave system are:

(*i*) the maximum electric field strength appearing within the system
(*ii*) the nature of the dielectric gas employed
(*iii*) the molecular density (or, equivalently, the absolute pressure and temperature) of the dielectric gas
(*iv*) the microwave frequency
(*v*) the breakdown volume.

Free electrons which always exist within the gas because of cosmic radiation and other random phenomena are accelerated by the electric field present and suffer collisions with neutral gas molecules. If the kinetic energy imparted to an electron by the field exceeds the ionization potential of the gas, the possibility exists of producing an additional electron upon collision with a neutral gas molecule. If the kinetic energy of the accelerated electron is less than the ionization potential, it may become attached to a neutral gas molecule upon collision. Diffusion produces a net flow of electrons from regions of high electronic density to regions of lower density. Some recombination of electrons and positive ions also occurs.

Breakdown occurs when the rate of electron production via ionization exceeds the combined rate of electron loss through the processes of attachment, diffusion, and recombination. For most high power transmission systems, the gas pressure is in the region of one to two atmospheres, and recombination rates are negligibly small. Also, since the dimensions of the breakdown volume are generally much greater than the characteristic diffusion length of the gas, electron loss via diffusion is also negligible. Hence, breakdown occurs when the rate of ionization exceeds the rate of attachment.

Both ionization and attachment rates are functions of the mean

electron energy[3] which, in the high pressure regime where collision frequency is far larger than the microwave frequency, is dependent on the ratio of the peak electric field strength (E) to the gas molecular density (N). Assuming the density is defined by the ideal gas law, the field strength at breakdown is given by

$$E = C\frac{\rho}{KT} \tag{1}$$

where

ρ = absolute gas pressure
K = Boltzman's constant
T = absolute temperature
C = constant, dependent upon dielectric gas

For SF_6, C = 3.69×10^{-19} volt-meter^2/molecule.

For irregularities in the waveguide such as those which occur at flanges, in hybrids, etc., the local voltage gradient is increased by a field enhancement factor (β). Substituting into (1) the waveguide field strength required for breakdown becomes

$$E = \frac{C\rho}{\beta KT}. \tag{2}$$

The electric field strength generated in a rectangular waveguide transmitting a power P can be shown to be

$$E^2 = \frac{4Z_oP}{d_1d_2} \tag{3}$$

where d_1 and d_2 are the waveguide cross-section dimensions and Z_o is the wave impedance. Therefore, the breakdown power threshold can be derived from (2) and (3) as

$$P = \left(\frac{d_1d_2}{4Z_o}\right)\left(\frac{C^2}{\beta^2K^2T^2}\right)\rho^2. \tag{4}$$

For constant temperature, this is the familiar relationship between peak power breakdown and the square of the absolute pressure, known to be valid in the high-pressure region where electron loss by diffusion is negligible.

III. EFFECTS OF HIGH AVERAGE POWER

The relationship discussed above has been understood and effectively applied for many years. However, in the experimental work described

below, a significant reduction in peak breakdown power was observed as the average power increased. It is noted that, although eq. (4) is not explicitly dependent upon average power, temperature does appear. Hence, it was postulated that loose particulate matter was reducing the breakdown power level because a loose particle is not thermally attached to the waveguide wall; its temperature therefore increases as the average power increases. This causes a reduction in the molecular density of the gas at the location of the particle, thereby reducing the field strength needed to cause breakdown. The presence of a particle also produces localized field enhancement. These two localized effects combine to lower the breakdown power.

The electric field enhancement factor and the equations for temperature rise at various levels of average power are derived in Appendix A for spherical conducting particles. This derivation neglects intrapulse heating since, within the range of pulse lengths investigated, it is negligible compared to average power heating. Using these results and eq. (4), peak power breakdown levels can be calculated for various average power levels and particle sizes. Figure 1 shows the results of such calculations for WR-284 waveguide filled with SF_6 at 25 psig containing spherical copper particles from 4 to 120 microns in diameter. Also appearing on Fig. 1 are experimental points obtained by introducing copper spheres of known diameter into a traveling wave resonator[4] constructed of high-conductivity copper to minimize losses. Correlation between theory and experiment is seen to be good.

It is observed from Fig. 1 that, within the range of particle sizes investigated:

(*i*) Peak breakdown power levels at very low levels of average power are independent of particle size and are below that of ideal waveguide because of field enhancement only.

(*ii*) As the average power increases, the presence of heated particles causes further reduction in power handling capability due to localized reduction in gas density. Larger particles cause a greater reduction in power handling capability because they are heated to higher temperatures.

The analysis from which Fig. 1 was derived is applicable when the particle dimensions are small compared with the waveguide dimensions, and large compared with the characteristic diffusion length of the gas. It should not be inferred from Fig. 1 that particle-induced arcing cannot occur above 100 megawatts, since particles with dimensions smaller than the diffusion length will cause breakdown to occur above this level. An analysis of particle behavior in this region was not considered.

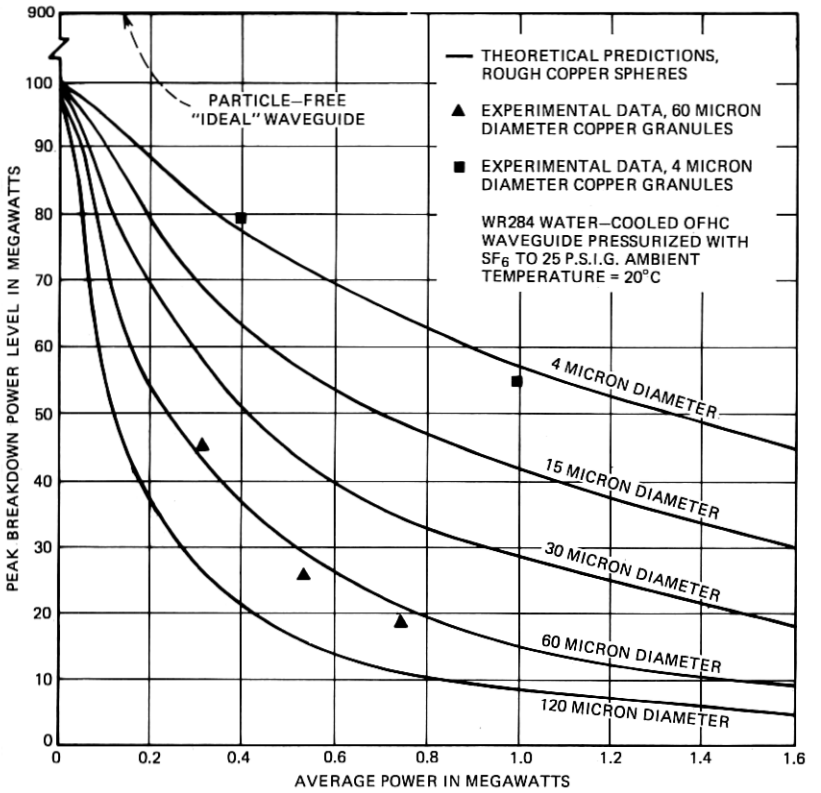

Fig. 1—Effect of particles on breakdown.

IV. EXPERIMENTAL WORK

The equipment used to obtain the experimental data is shown in schematic form in Fig. 2. A resonant ring was used to generate the high power levels required to produce breakdown with the RF power source available. A photograph of the equipment is shown in Fig. 3. View ports were provided to permit visual observation of arcing. Thermocouples were inserted in flanges and attached to the waveguide in various places to monitor temperature rise versus average power. Forward and reverse power was monitored by power meters and by oscilloscopes. A counter was used to record the number of arcs.

Because of the high average power levels, the waveguide was water-cooled. Two cooling channels were soldered on the top and bottom walls through which water was circulated at a rate of 7 gallons per minute. To permit assembly of the flange bolts, the cooling channels were

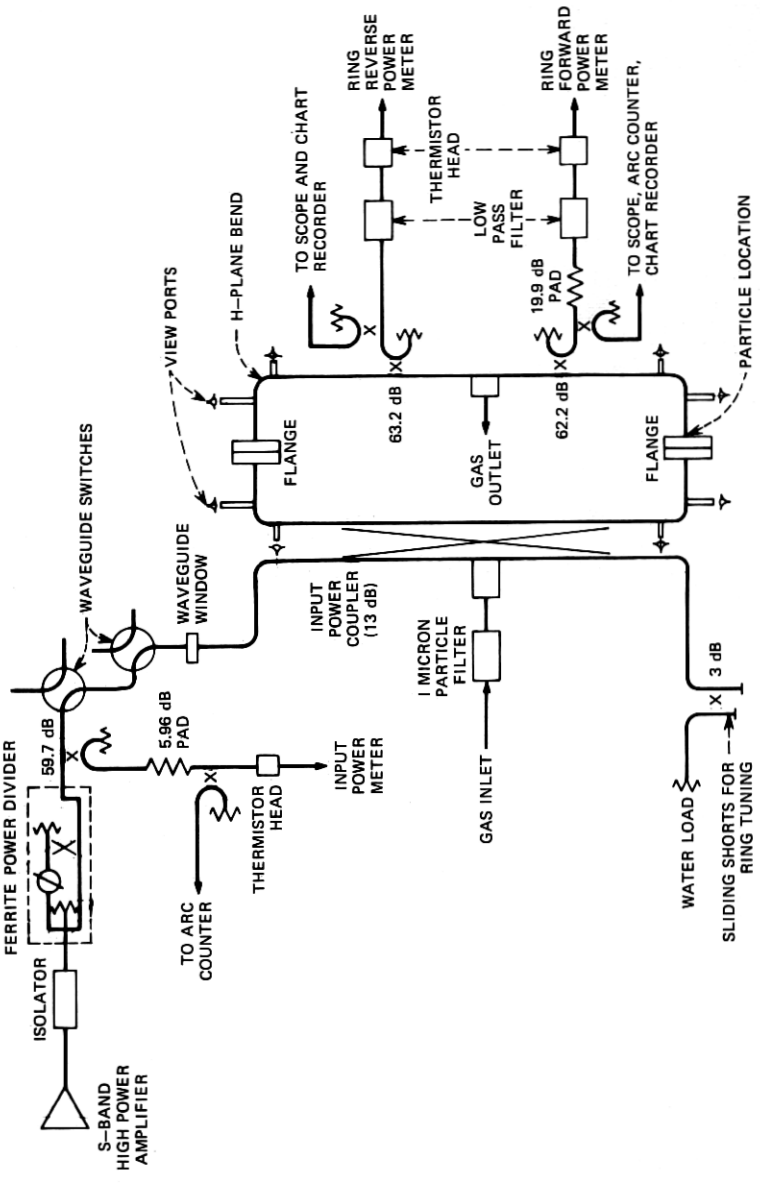

Fig. 2—Resonant ring experimental setup.

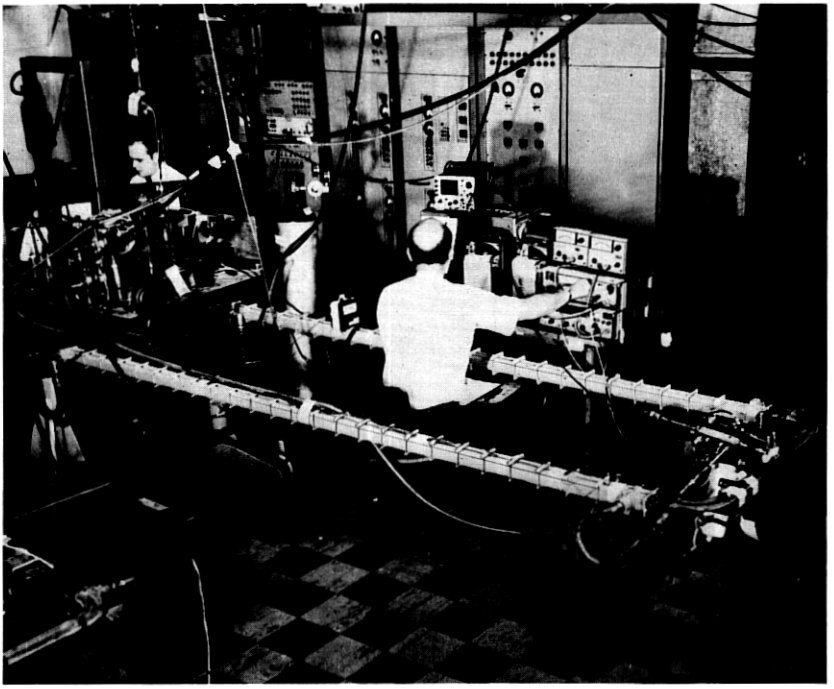

Fig. 3—Resonant ring.

terminated 2-1/2 inches from the flange. Because of this, the flange temperature was found to rise at a rate of 65°C/megawatt of average power. This factor has been included in the particle temperature calculations of Appendix A. The flange used was adapted from a vacuum-tight design, the principle feature of which was the use of a stainless steel knife edge and a soft copper gasket to provide the RF and gas seal. Figure 4 shows a model of the flange and cooled waveguide.

V. RF PROCESSING

Early experience with the setup described above showed arcing at substantially lower peak power levels than expected. By use of the viewports, it was observed that many arcs were being initiated at the power coupler and monitoring coupler slots. These were attributed to high gradients at sharp corners. By allowing arcing to continue, the test setup was "aged" to progressively higher and higher peak and average powers. When arcing no longer occurred at these points, it was observed

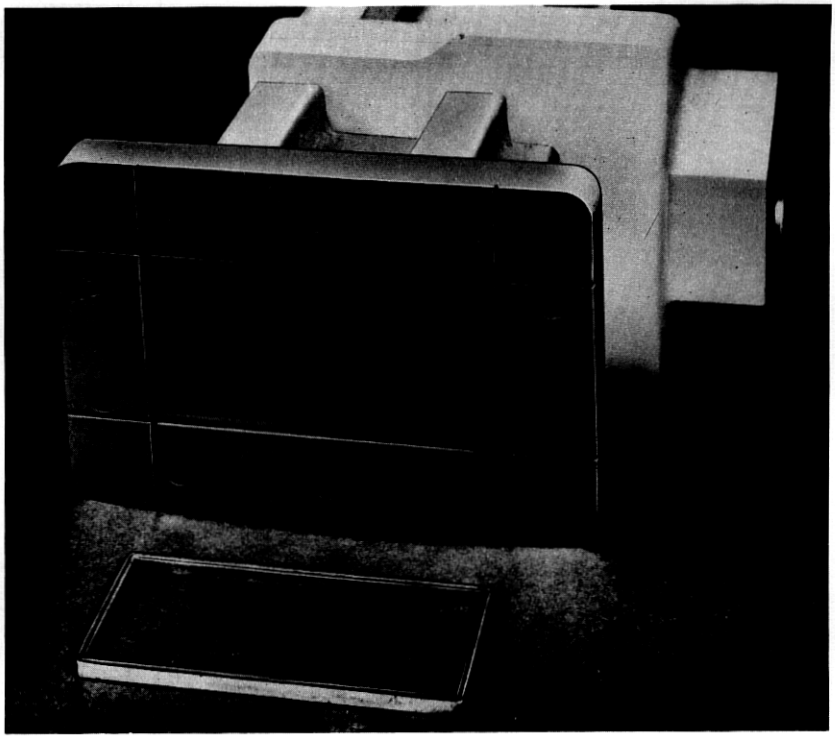

Fig. 4—Flange.

to occur at randomly located places, becoming more intense at higher levels of average power. This observation was a factor in generating the hypothesis that particulate matter was inducing breakdown. The average power limitation imposed by the particulate matter was experimentally found to be lessened by allowing the arcing to continue until stopped, a procedure which came to be known as "processing."

As shown in Fig. 1, when a high average power is present, very small particles can cause arcing at levels well below the inherent peak power handling capability of the system. Processing is accomplished by applying power to the assembled system, increasing the power levels until breakdown is induced by the particles and then waiting until arcing subsides. Processing arcs change the physical configuration of the initiating particles by (*i*) breaking them into smaller particles, (*ii*) removing them from the high field region via breakdown pressure waves, and/or (*iii*) vaporization. Figure 1 shows that, as the particles

become smaller, a higher peak power can be handled before arcing occurs. Therefore, by raising the power level in discrete steps and remaining at each level for a period of time sufficient to allow processing to occur, the power-handling capability of the microwave system increases to a higher value. This value can be maintained as long as the system is intact, that is, not opened. Disassembly always introduces particulate matter and some reprocessing is required to achieve the former stable power handling level.

Figure 5 shows an experimental processing sequence. The data was taken in a 10-foot ring set up as shown in Fig. 2. Parameters for this experiment were:

Pulse length—120 microseconds
Dielectric gas—SF_6 at 25 psig
Ambient temperature—28°C.

The charts appearing in Fig. 5 depict the number of arcs which occurred in two-minute intervals at the indicated power levels. In all tests, duty cycle was varied by holding the pulse length fixed and changing the pulse repetition rate. Arcing began during Run 1 at a peak power level of 12.6 megawatts with a 1.5 percent duty cycle. It is noted that (*i*) each time the power levels were raised to higher values, breakdown occurred, and (*ii*) at each power level, the number of arcs which occurred per two-minute interval decreased with time. At and above the peak power level of 66.7 megawatts, the average power was held constant at 1 megawatt. Performance became unstable at the peak power level of 139 megawatts.

Run 2 was then executed. It is noted that the processing arcs which occurred during Run 1 improved system performance to the extent that during Run 2, no discharges occurred below the power levels of 66.7-megawatts peak, 1-megawatt average. Also, fewer arcs occurred at the higher power levels than during Run 1. Performance became unstable at a power level of 151 megawatts peak. The results of this experiment demonstrate that processing a system to a high power level raises the power level at which subsequent discharges occur and reduces their severity.

Ideally, processing should be performed at power levels exceeding system requirements so that operation at the design power levels would be virtually arc-free. Such a procedure cannot be applied to a typical system which normally operates at the maximum available power level. Processing can still be applied in such a situation, however, if it is performed with the dielectric strength of the gaseous fill somehow reduced. This can be accomplished either by introducing a low dielectric

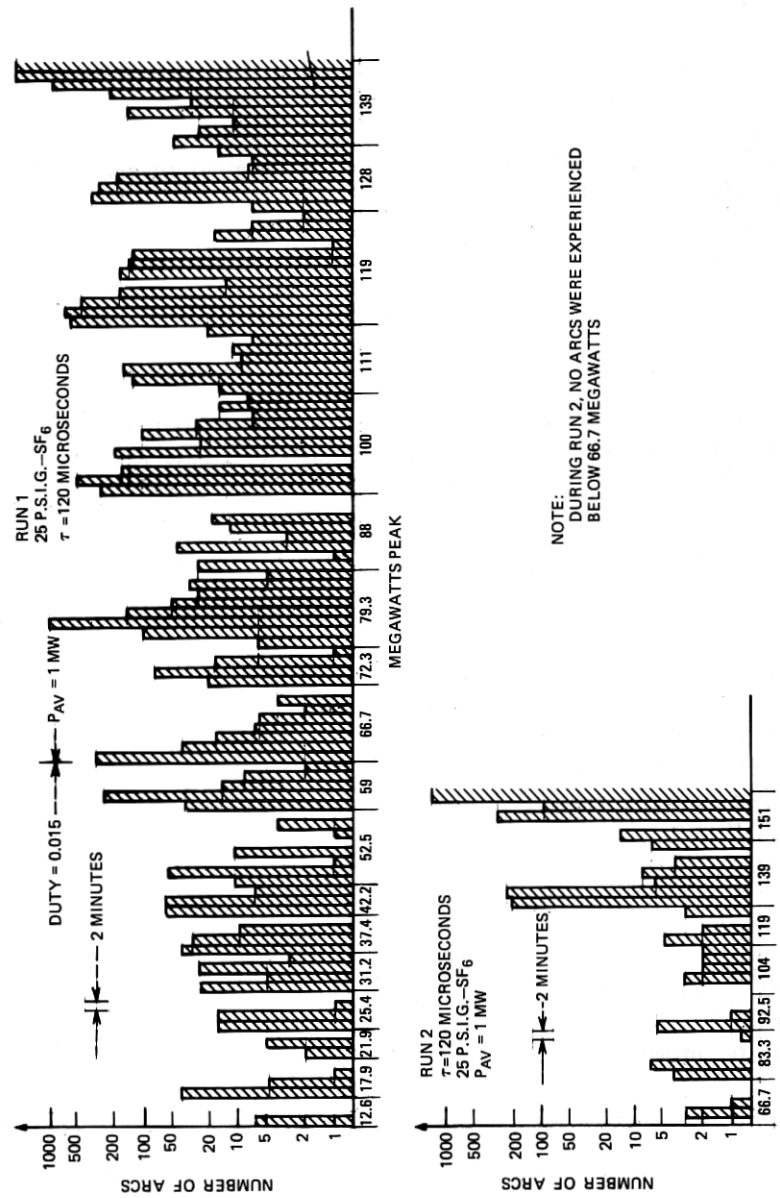

Fig. 5—Waveguide processing.

strength gas before processing, or by processing with the pressure of the normal dielectric gas reduced. Processing can then occur to a greater extent with the available power and will result in stable performance when the system is operated with normal dielectric strength.

Dry nitrogen was first investigated as a processing agent because of its low dielectric strength. It was found that after the initiation of a processing arc, nitrogen does not recover its dielectric strength sufficiently fast to prevent breakdown on all successive pulses. Hence, processing cannot be satisfactorily performed using this gas.

Processing with low pressure SF_6 was next investigated. A 32-foot resonant ring was selected for this purpose. Results are shown in Fig. 6. The ring was processed to power levels of 20 megawatts peak, 700 kilowatts average while filled with SF_6 at a pressure of 5 psig. After increasing the gas pressure to 25 psig, the peak power level was raised with the average power held constant; breakdown did not again occur until a peak power level of 35 megawatts had been achieved. Hence, processing with 5 psig of SF_6 provided almost 3 dB of margin in power handling capability when the system was repressurized to 25 psig. This data was successfully repeated after disassembly and reassembly of the structure. Hence, reduced pressure SF_6 can be employed in the processing of a practical system to assure some power handling margin.

VI. PROCESSING CONSIDERATIONS AND LIMITATIONS

The energy dissipated by processing arcs must be kept sufficiently low to prevent the temperature rise of the waveguide surface in the vicinity of the arc from exceeding the melting point of the waveguide material. If melting of the waveguide wall occurs, the turbulence of the arc can eject small masses of molten metal into the waveguide interior, preventing processing since the additional particles induce continuing breakdown. Hence, the arc rate, instead of subsiding with time, increases. Such a situation is referred to as massive breakdown and is evident in Fig. 5, Run 2 at the 151-megawatt level.

It will be shown that the power level at which massive breakdown occurs is inversely proportional to the square root of the time duration of a single arc. To analyze the effects of arc duration upon waveguide processing, it is necessary to determine (*i*) the formative time of a processing arc, and (*ii*) the percentage of incident power absorbed by a growing arc as a function of time. The processes contributing to the growth of an arc which begins at the surface of a small particle have not, to the authors' knowledge, been investigated in any depth. In our

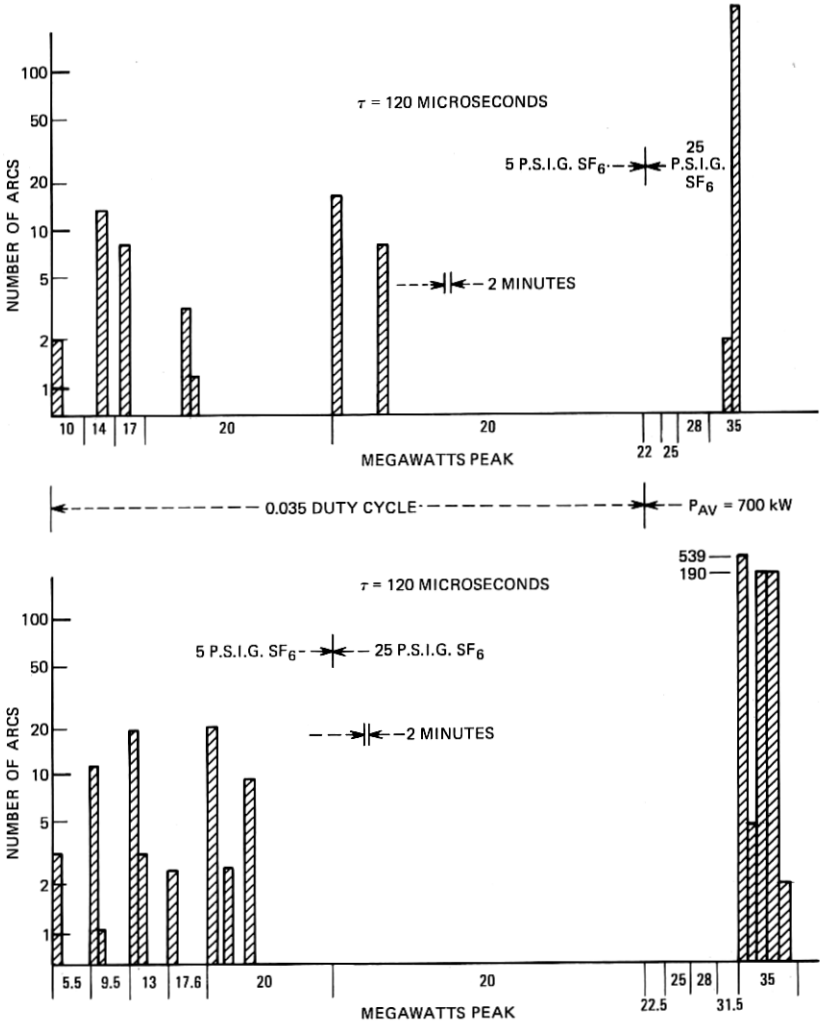

Fig. 6—Low-pressure processing.

investigation, no rigorous analytical determination of the desired two quantities was attempted; rather, both were determined experimentally. The experimental procedure is contained in Appendix B. The waveforms observed suggest that the power absorbed by a processing arc when the incident power is constant can be approximated by the form:

$$P_A = \alpha[1 - e^{-t/T}]P_o \tag{5}$$

where

P_o = incident power
T = formative time constant of the arc, independent of power level
α = steady-state absorption percentage.

For WR-284 waveguide pressurized to 25 psig with SF_6, it was found that $T = 2$ microseconds and $\alpha = 1.5$ percent.

The rise in temperature of the waveguide wall in the vicinity of a processing discharge can be determined by assuming that the thermal conductivities and heat capacities of the dielectric gas and the waveguide material are such that power dissipated within an arc is transferred instantaneously to the waveguide walls. Consider the semi-infinite block of metal shown in Fig. 7. Let $P_A(t)$ be the power per unit area at the metal surface $x = 0$. It can be shown[5] that the temperature rise within the metal for $t > 0$ is given by:

$$\Delta T = \frac{\gamma}{2} \int_0^t \frac{P_A(u)}{\sqrt{t-u}} e^{-[x^2/4(t-u)]}\, du \tag{6}$$

where u is a dummy variable of integration and γ is a constant dependent upon the thermal conductivity and heat capacity of copper. At the

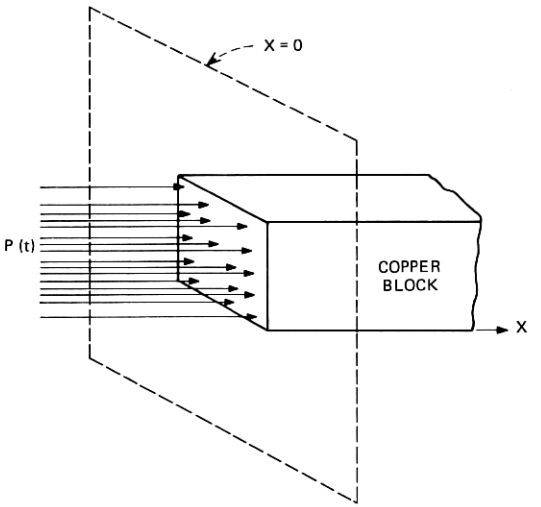

Fig. 7—Model employed to calculate ΔT.

surface of the metal, $x = 0$, this integral becomes:

$$\Delta T = \frac{\gamma}{2} \int_0^t \frac{P_A(u)}{\sqrt{t-u}}\, du. \tag{7}$$

The power absorbed by an arc is given by eq. (5). Consequently, by substituting (5) in (7), the temperature rise of the waveguide surface at time t after the arc is initiated is found to be:

$$\Delta T = \frac{\gamma}{2} \int_0^t \frac{\alpha[1 - e^{-t/T}]P_o/A}{\sqrt{t-u}}\, du \tag{8}$$

where A is the cross-sectional area of the arc.

For our situation, the arc duration, t, exceeds the arc formative time constant, T, so that:

$$\Delta T(o, t) \cong \frac{\alpha\gamma}{2} \frac{P_o}{A} \int_0^t \frac{1}{\sqrt{t-u}}\, du \tag{9a}$$

or

$$\Delta T \cong \frac{\gamma\alpha}{A} P_o \sqrt{t}. \tag{9b}$$

Therefore, the temperature rise experienced at the waveguide wall varies as the square root of arc duration, t. To prevent the waveguide wall temperature from exceeding the melting point of the waveguide material, the arc duration, t, must be kept small.

To test the validity of the above theory of processing limitation resulting from particle generation, processing was performed within WR-284 resonant structures of various lengths, pressurized with SF_6 at 25 psig. The duration of an arc which occurs within a resonant structure is determined by the time required to dissipate all of the energy which was stored within the resonator prior to breakdown. Since stored energy increases with resonator length, arc duration also increases with resonator length.

Whereas the incident power in a terminated line is a constant, the power incident upon an arc in a resonant structure decreases with time as the stored energy is consumed by the arc. An expression for this incident power as a function of time $P_o(t)$ is derived in Appendix B (eq. 60). The power absorbed by the arc is therefore:

$$P_A(t) = \alpha P_{F_o}(1 - e^{-t/T}) \exp\left\{-\frac{v_o\alpha}{l}[t - T(1 - e^{-t/T})]\right\} \tag{10}$$

where

P_{F_e} = resonator equivalent power level prior to breakdown
v_g = group velocity of electromagnetic wave within the resonator
l = resonator length.

Substituting this value of absorbed power into equation (6) yields:

$$\Delta T = \frac{\gamma}{2A} \int_0^t \frac{\alpha(1 - e^{-u/T}) \exp \{-(v_g/l)\alpha[u - T(1 - e^{-u/T})]\} P_{F_e}}{\sqrt{t - u}}. \quad (11)$$

Experimental verification of these relationships was accomplished on four resonant structures. The first two were waveguide cavities with input and output irises designed for optimum power multiplication. The other two were resonant ring structures. All structures were pressurized with SF_6 at 25 psig and processed as described above to the point of massive breakdown. The results are as shown in Table I.

Resonators 1 and 3 were operated at a constant 0.5-percent duty cycle. Resonators 2 and 4 were operated with the average power held constant at 1 megawatt. The massive breakdown power reached is noted. The last column is the calculated value of the relative wall temperature reached at massive breakdown using eq. 11. The calculations were performed numerically on a digital computer and are plotted in Fig. 8.

These calculated maximum values are relatively close, in spite of the fact that the structures are radically different in dimensions. The calculated wall temperature rise of the short resonator deviates most. This is probably because the power level at which breakdown occurred was relatively close to the theoretical breakdown limit of the waveguide which is 900 megawatts. These experimental data imply that massive breakdown occurs when the rise in waveguide surface temperature above ambient operating temperature exceeds a critical value of approximately 850 γ/A.

A microscopic examination of some of the parts used in these experiments confirmed the analysis. Arc marks were found to be present upon

TABLE I—BREAKDOWN POWER LEVEL VERSUS LENGTH

No.	Resonator Length (Meters)	Massive Breakdown Power Level (Megawatts)	ΔT Maximum
1	0.135	650	675 γ/A
2	3.05	150	875 γ/A
3	3.66	150	895 γ/A
4	9.65	70	960 γ/A

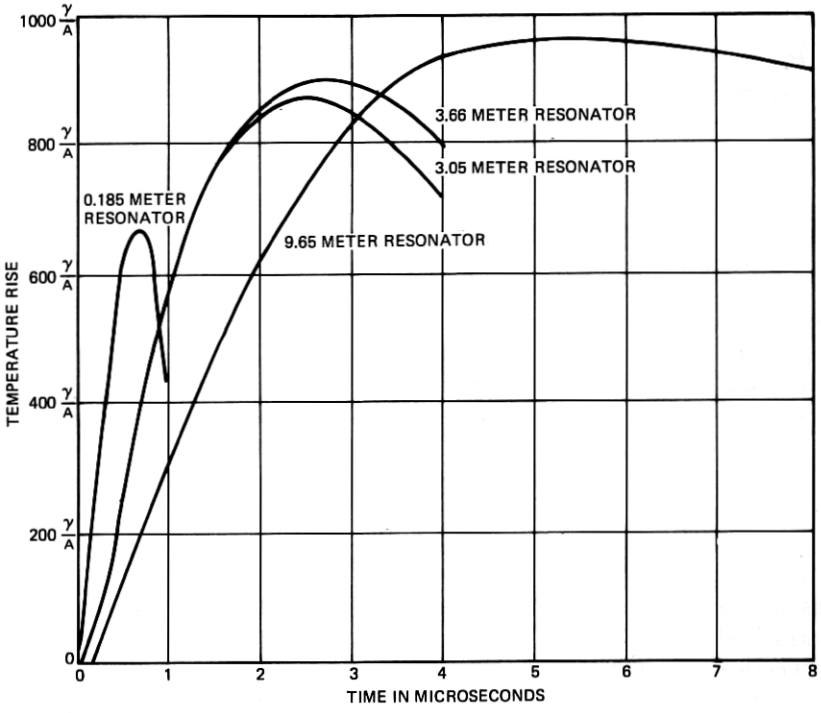

Fig. 8—Waveguide surface temperature rise during massive breakdown arcs.

the waveguide flange gaskets which were removed from the 10-foot and 38-foot resonant rings after massive breakdown. One such arc mark, magnified approximately 200 times is shown in Fig. 9. To achieve proper lighting, it was necessary to tilt the gasket under the microscope. Hence, only a thin horizontal strip is in focus. It is noted that the arc mark consists of an area of discoloration approximately 6 millimeters in diameter, and that a small hemispherical crater approximately 30 microns in diameter is located near the center of the discoloration. The area of discoloration is believed to have been caused by excessive heating, and the crater formed after the waveguide wall had melted. Referring to Fig. 1, it is obvious that the size of the conducting particle removed from the crater is capable of initiating additional discharges. The size of the particle generated is consistent with values reported for particles formed by dc discharges of roughly the same energy as experienced at massive breakdown in the resonators.[6]

Processing considerations in a practical system based upon the above

theory of particle generation and massive breakdown can be illustrated by the following example. Suppose a microwave system is to be designed to transmit 20 megawatts of peak power with 60-microsecond pulses, and that after 10 microseconds of a pulse has elapsed, an arc is initiated by a particle of suitable size. The arc duration is therefore 50 microseconds, and eq. (9b) predicts a temperature rise of:

$$\Delta T = \frac{\gamma\alpha}{A} \times 20 \times 10^6 \sqrt{50 \times 10^{-6}} = 141 \times 10^3 \frac{\alpha\gamma}{A}.$$

For SF_6, $\alpha = 1.5 \times 10^{-2} \Rightarrow \Delta T = 2100\,\gamma/A$. Hence, melting occurs, and massive breakdown will ensue. If, however, the initiation of the arc was detected (such as by comparing forward power levels at the amplifier and at the load) and the RF drive was blanked within, say, 4 microseconds after arc initiation, then:

$$\Delta T = \frac{\gamma\alpha}{A} \times 20 \times 10^6 \sqrt{4 \times 10^{-6}} = 40 \times 10^3 \alpha\gamma/A.$$

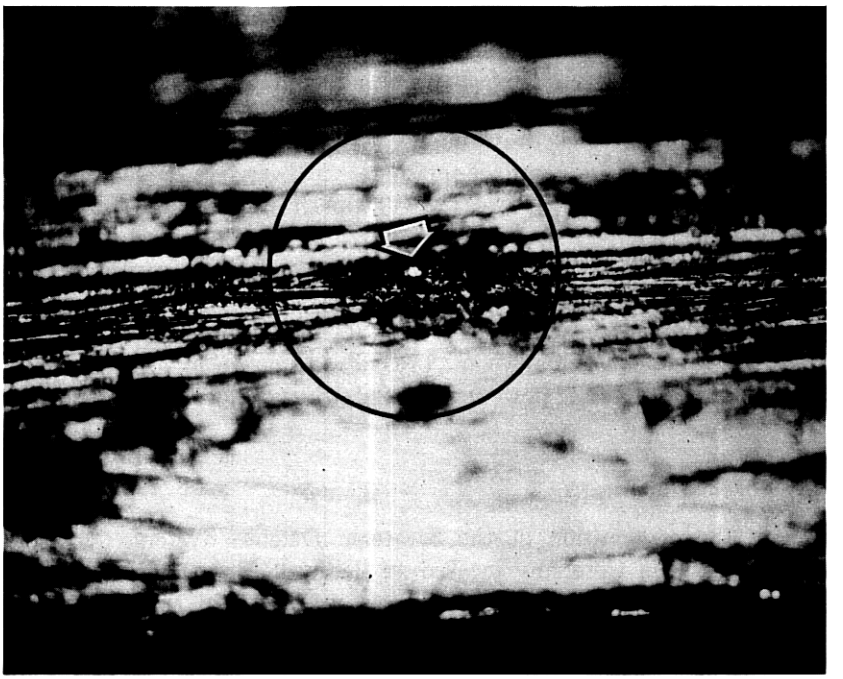

Fig. 9—Arc mark.

For $\alpha = 1.5 \times 10^{-2}$, $\Delta T = 600\,\gamma/A$. Thus, by employing this "early-off" protection, the critical temperature is not exceeded, and processing can be carried to completion in a high average power system.

VII. CONCLUSION

The theoretical and experimental investigation of the effects of high average power levels and long pulse lengths on waveguide breakdown has shown that:

(*i*) Loose particulate matter (e.g. thermally detached from the waveguide wall) is heated to high temperatures by high levels of average power. The resulting rarification of the dielectric gas in the vicinity of the heated particle, coupled with field enhancement at the particle boundary, causes breakdown to occur at values of peak power below that expected in the absence of particles.

(*ii*) Waveguide "processing" with RF discharges of short duration can be used to eliminate undesirable foreign matter and increase the power handling capability of a microwave system.

(*iii*) To achieve processing, arcs must terminate as soon as possible after they occur by blanking the remainder of the RF pulse. This prevents excessive energy dissipation in the arc which can cause waveguide surface melting.

(*iv*) The ultimate peak power level to which a system can be processed varies inversely with the square root of the allowed arc duration.

(*v*) Processing requires a dielectric gas which rapidly recovers its dielectric strength. Sulphur hexafluoride is ideal and perhaps the only practical choice. With its use, processing at reduced pressure can achieve some breakdown margin in the usual case where processing power is limited to the normal operating power.

VIII. ACKNOWLEDGMENTS

With the cooperation of the Strategic Defense Systems Division of the Raytheon Company located at Bedford, Massachusetts, much assistance was given and most of the data was taken by the Equipment Division of the Raytheon Company located at Wayland, Massachusetts. Miss Patricia Loth of the Hazeltine Corporation, Long Island, New York also contributed to the planning and conduct of the experiments.

APPENDIX A

Field Enhancement and Heating of Conducting Particles

Consider a spherical conducting particle located within a waveguide as shown in Fig. 10a. For simplicity, the particle is assumed to be centrally located and completely detached from any of the waveguide walls. When electromagnetic waves are propagated through the waveguide, the boundary conditions imposed by the particle cause the field to be distorted. Since the radius of the particle is much less than a wavelength, the quasi-static approximation can be applied to obtain a good estimate of the fields existing in the vicinity of the particle. The models shown in Figs. 10b and 10c will be used to obtain the quasi-static fields. The coordinate systems used in Figs. 10b and c are unrelated to each other or to that of Fig. 10a. The zero-order longitudinal magnetic field can be neglected, since the particle is assumed to be centrally located (H_z is zero at the center of the waveguide transverse section for the mode of interest, namely the TE_{10}).

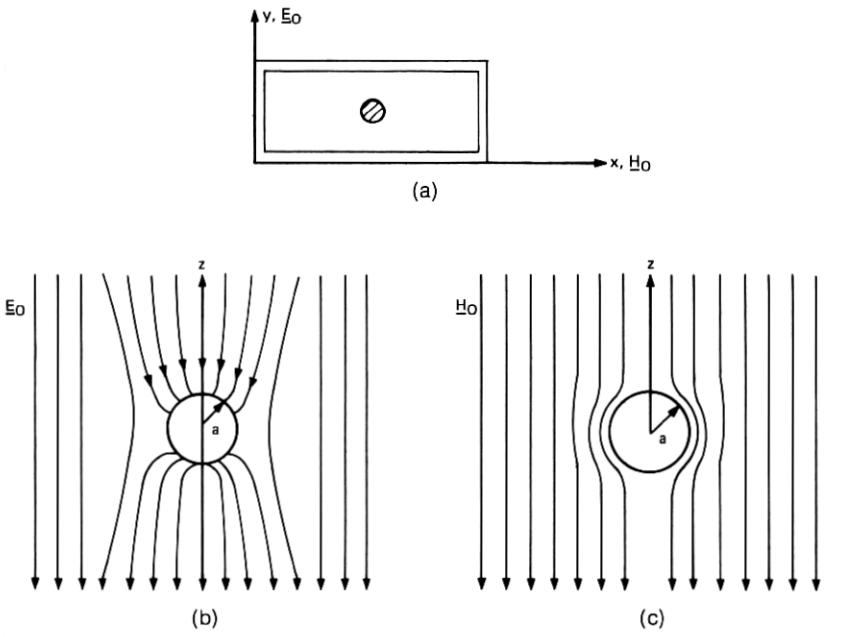

Fig. 10—Particle model: (a) Particle location. (b) E field model. (c) H field model.

The quasi-static approximation consists of expressing the total electromagnetic field in the form:

$$\mathbf{E} = \mathbf{e}_0 + \omega\mathbf{e}_1 + \omega^2\mathbf{e}_2 + \cdots \tag{12}$$

$$\mathbf{H} = \mathbf{h}_0 + \omega\mathbf{h}_1 + \omega^2\mathbf{h}_2 + \cdots \tag{13}$$

where

$$\nabla \times \mathbf{e}_0 = 0 \tag{14}$$

$$\nabla \times \mathbf{h}_0 = 0 \tag{15}$$

$$\omega\nabla \times \mathbf{h}_1 = +\epsilon_0 \frac{\partial \mathbf{e}_0}{\partial t}$$

$$\omega\nabla \times \mathbf{e}_1 = -\mu_0 \frac{\partial \mathbf{h}_0}{\partial t}$$

$$\vdots$$

$$\omega\nabla \times \mathbf{h}_n = +\epsilon_0 \frac{\partial \mathbf{e}_{n-1}}{\partial t} \tag{16}$$

$$\omega\nabla \times \mathbf{e}_n = -\mu_0 \frac{\partial \mathbf{h}_{n-1}}{\partial t}. \tag{17}$$

The approximation consists of truncating (12) and (13) after a sufficient number of terms. The zeroth order fields $\mathbf{e}_0$ and $\mathbf{h}_0$ are found from eqs. (14), (15) and the unperturbed fields E_0 and H_0.

The magnitudes of the higher-order correction fields are related to the magnitudes of the zeroth order fields by the factor $(a/\lambda)^n$, where λ is the wavelength, a is a characteristic dimension of the perturbation, and n is the index of the correction field being considered. Since $a \ll \lambda$, it follows that the first and all higher-order correction fields can be neglected, and the fields in the vicinity of the particle are closely approximated by the zeroth-order terms. These are found by solving LaPlace's equation in spherical coordinates for the electric and magnetic scalar potentials, taking the gradients of these functions, and applying the boundary conditions $\mathbf{e}_0 \mid_{r\to\infty} = -E_0\mathbf{i}_z$; $e_{0\theta} \mid_{r=a} = 0$, $\mathbf{h}_0 \mid_{r\to\infty} = H_0\mathbf{i}_z$; $h_{0r} \mid_{r=a} = 0$. The results are:

$$\mathbf{e}_0 = -E_0\left[1 + 2\left(\frac{a}{r}\right)^3\right]\cos\theta\mathbf{i}_r + E_0\left[1 - \left(\frac{a}{r}\right)^3\right]\sin\theta\mathbf{i}_\theta \tag{18}$$

$$\mathbf{h}_0 = H_0\left[1 - \left(\frac{a}{r}\right)^3\right]\cos\theta\mathbf{i}_r - H_0\left[2 + \left(\frac{a}{r}\right)^3\right]\sin\theta\mathbf{i}_\theta . \tag{19}$$

Now, from eq. (18), it follows that $\mathbf{e}_0$ assumes its maximum value at $\theta = 0$, $r = a$. This value is:

$$| \mathbf{e}_0 |_{\max} = 3E_0 . \tag{20}$$

Hence, the field enhancement factor, β, for spherical conducting particles is 3.

From eq. (19),

$$\mathbf{h}_0 |_{r=a} = -3H_0 \sin \theta \mathbf{i}_\theta \tag{21}$$

$$| I_s | = | \mathbf{h}_0(a) | = 3H_0 \sin \theta \tag{22}$$

where I_s is the surface current density induced in the particle by the field. If the microwave frequency is high enough such that the skin depth of penetration into the particle is much less than the particle's radius, the surface current density may be assumed to flow uniformly within one skin depth, δ. Hence, the current density J becomes:

$$\mathbf{J} = \frac{I_s}{\delta}. \tag{23}$$

The power dissipated per unit volume within one skin depth of the particle is therefore:

$$P_V = \frac{1}{2} \frac{| J |^2}{\sigma} = \frac{1}{2} \frac{| I_s |^2}{\sigma \delta^2} \tag{24}$$

where σ is the conductivity of the particle. The power dissipated per unit surface area of the particle therefore becomes:

$$P_A = \delta P_V = \frac{| I_s |^2}{2\sigma\delta}. \tag{25}$$

But

$$\delta = \sqrt{2/\omega\mu_0\sigma} \tag{26}$$

$$\therefore \quad P_A = \frac{| I_s |^2}{2} \sqrt{\frac{\omega\mu_0}{2\sigma}} \tag{27}$$

or

$$P_A = \frac{9H_0^2 \sin^2 \theta}{2} \sqrt{\frac{\omega\mu_0}{2\sigma}}. \tag{28}$$

The total dissipated power becomes:

$$P_{\text{diss}} = \int P_A \, dS \tag{29}$$

$$= \int_0^\pi \int_0^{2\pi} \frac{9H_0^2}{2} \sqrt{\frac{\omega\mu_0}{2\sigma}} a^2 \sin^3 \theta \, d\theta \, d\phi \tag{30}$$

or

$$P_{\text{diss}} = \frac{36H_0^2a^2}{3}\sqrt{\frac{\omega\mu_0}{2\sigma}}. \tag{31}$$

But the propagating power level, P, is related to H_0 by the expression

$$P = \frac{d_1d_2Z_0}{4}H_0^2 \tag{32}$$

where Z_0 is the TE_{10} wave impedance.

$$\therefore \qquad P_{\text{diss}} = \frac{144\pi a^2\sqrt{\frac{\omega\mu_0}{\sigma}}}{3Z_0d_1d_2}P. \tag{33}$$

Since

$$Z_0 = \sqrt{\frac{u_0}{\epsilon_0}}\frac{\omega/c}{\sqrt{(\omega/c)^2 - (\pi/d_1)^2}}, \tag{34}$$

$$P_{\text{diss}} = \frac{144\pi a^2}{3d_1d_2}\sqrt{\frac{\omega\epsilon_0}{2\sigma}}\left[1 - \left(\frac{c\pi}{d_1\omega}\right)^2\right]P \tag{35}$$

where c is the free-space velocity of light.

To calculate the temperature rise of the particle resulting from this dissipated power, let $\mathbf{n}$ be the heat flux density flowing from the particle:

$$\oint_{\substack{\text{particle}\\ \text{surface}}} \mathbf{n}\cdot d\mathbf{A} = P_{\text{diss}}. \tag{36}$$

Now, assuming heat flow by conduction through the gas,

$$\mathbf{n} = -\xi\nabla T \tag{37}$$

where ξ is the thermal conductivity of the gas. In the steady-state, conservation of energy implies that:

$$\nabla\cdot\mathbf{n} = 0 \tag{38}$$

$$\therefore \qquad -\nabla\cdot[\xi\nabla T] = 0. \tag{39}$$

For SF_6,[7]

$$\xi \cong \xi_o T \tag{40}$$

where $\xi_o = 4.3 \times 10^{-5}$ watts/meter-°K^2. Hence,

$$\xi_o\nabla\cdot[T\nabla T] = 0. \tag{41}$$

From circular symmetry, eq. (41) becomes

$$\frac{\xi_o}{r^2}\frac{d}{dr}\left[r^2 T \frac{dT}{dr}\right] = 0. \tag{42}$$

The solution of this differential equation is:

$$T = \sqrt{c_2 - \frac{c_1}{\xi_o r}} \tag{43}$$

where c_1, c_2 are constants determined by applying the boundary conditions

$$T\,|_{r\to\infty} = T_o\,, \qquad \int_{\substack{\text{particle}\\ \text{surface}}} \mathbf{n}\cdot d\mathbf{A} = P_{\text{diss}}\,.$$

The result is:

$$T = \sqrt{T_o^2 + \frac{P_{\text{diss}}}{2\pi\xi_0 r}}. \tag{44}$$

The absolute temperature of the particle, T_p, is therefore

$$T_p = T\,|_{r=a} = \sqrt{T_o^2 + \frac{P_{\text{diss}}}{2\pi\xi_0 a}} \tag{45}$$

where P_{diss} is given by eq. (35). It is observed that P_{diss} is dependent upon the electrical conductivity, σ, of the particle.

Since the electrical conductivity of a conductor varies inversely with the absolute temperature,

$$\sigma = \sigma_o \frac{T_p}{T_A} \tag{46}$$

where T_A is the ambient temperature and is assumed to be 293°K and σ_o is the conductivity at ambient temperature. For copper, the bulk conductivity is equal to 5.5×10^7 meters/ohm. Because microwave current densities flow within a narrow skin depth, ripples in the surface of the conductor cause a decrease in the effective conductivity near the surface.[8] At S-band frequencies, surfaces with rms variations on the order of several skin depths (such as rough spheres) have an effective conductivity of approximately 62 percent of the bulk conductivity. Hence, a value of 3.44×10^7 meters/ohm will be assumed for σ_o when calculating the temperatures of the copper spheres.

Substituting eqs. (35) and (46) into (45) yields:

$$T_p = \sqrt{T_o^2 + \frac{72aP_{av}\sqrt{\frac{T_p\omega\epsilon_o}{2}\left[1 - \left(\frac{c\pi}{d_1\omega}\right)\right]}}{3d_1d_2\xi_o\sqrt{\sigma_oT_A}}}. \tag{47}$$

Letting

$$B = \frac{72\sqrt{\frac{\omega\epsilon_o}{2}\left(1 - \frac{c\pi}{d_1\omega}\right)^2}}{3d_1d_2\xi_o\sqrt{\sigma_oT_A}} \tag{48}$$

yields:

$$T_p^2 = T_o^2 + BaP_{av}\sqrt{T_p}\,. \tag{49}$$

Experimentally, $d_1 = 2.84$ inches, $d_2 = 1.34$ inches.

$$\therefore \qquad B = 4.68 \times 10^2 \text{ in MKS units}$$

Finally, T_o is equal to the temperature of the waveguide in the region where the particle is located. Experimentally, the particles were introduced at the waveguide flanges, and the flanges were found to experience a temperature rise of 65°C/megawatt of average power above ambient. Hence, to be consistent with experiment,

$$T_o = T_A + 65 \times 10^{-6}P_{av} \tag{50}$$

where T_A is the ambient room temperature (293°K). Hence,

$$T_p^2 = (293 + 65 \times 10^{-6}P_{av})^2 + 4.68 \times 10^2aP_{av}\sqrt{T_p}. \tag{51}$$

Values of T_p which satisfy (51) appear in Table II for various values of P_{av} and particle radius a.

APPENDIX B

Arc Formative Time and Power Absorption

The formative time of a processing arc is defined as the interval from arc initiation to complete interruption of power transmitted. Photographs of traveling-wave resonator waveshapes taken during the occurrence of processing arcs indicate that processing-arc formative times are independent of peak power level over the range of investigation (11 to 80 megawatts peak).

The formative time was measured within a terminated WR-284 system pressurized with SF_6 at 25 psig. Transmitted power pulses were

TABLE II—PARTICLE TEMPERATURE T_p AS A FUNCTION OF SIZE AND POWER LEVEL

Particle Radius (Microns)	Average Power (Watts)				
	10^5	2×10^5	4×10^5	8×10^5	1.6×10^6
60	388°K	478°K	648°K	960°K	1425°K
30	346°K	395°K	491°K	664°K	964°K
15	323°K	350°K	405°K	508°K	696°K
7.5	310°K	327°K	365°K	426°K	550°K
2	300°K	312°K	332°K	368°K	436°K

monitored on a storage oscilloscope at the termination. The formative time was found from the rate of decay of the transmitted power pulse whenever a discharge occurred at any point between the final power amplifier and the termination. A terminated (non-resonating) structure was employed for this measurement to divorce the arc formative time from the natural decay of a resonator caused by the additional arc loading. It was observed that the rate of decay of power transmitted past an arc was independent of the initiating power level and that the transmitter power waveshape decayed exponentially with a time constant of 2 microseconds. Hence, in WR-284 waveguide pressurized to 25 psig with SF_6, the power absorbed by an arc can be written as:

$$P_A = \alpha P_o[1 - e^{-t/T}] \tag{52}$$

where

t = time
P_o = incident power
α = steady-state percentage of incident power absorbed by arc
T = 2 microseconds.

The value of α was determined by use of a traveling wave resonator. When an arc is struck within a resonant structure, it begins to absorb the energy that was stored in the resonator and the fields decay to zero. The rate of decay of the fields is dependent upon the percentage of incident power absorbed by the arc. This relationship is derived as follows.

Let $P_F(t)$ be the instantaneous power level within the resonator; then, when an arc is initiated,

$$P_F(t + \tau) = [1 - a(t)]P_F(t) \tag{53}$$

where

τ = transit time through the resonator ($= l/v_g$ where l is the resonator length and v_g the group velocity)

$a(t)$ = percentage of incident power absorbed by arc as a function of time.

Since τ is small,

$$P_F(t + \tau) \cong P_F(t) + \tau \frac{dP_f}{dt}. \tag{54}$$

Substituting eqs. (52) and (54) into (53) yields

$$\tau \frac{dP_F}{dt} = -\alpha[1 - e^{-t/T}]P_F \tag{55}$$

$$\Rightarrow P_F = C \exp \{-\alpha/\tau[t + Te^{-t/T}]\}. \tag{56}$$

Now,

$$P_F(t = 0) = P_{F_0} \tag{57}$$

$$\Rightarrow P_F = P_{F_0} \exp \{-\alpha/\tau[t - T(1 - e^{-t/T})]\}. \tag{58}$$

But

$$e^{-t/T} \cong 1 - \frac{t}{T} + \frac{t^2}{2T^2} \tag{59}$$

$$\therefore \quad P_F \cong P_{F_0} \exp \{-\alpha/\tau[t - T(1 - 1 + t/T - t^2/2T)]\} \tag{60}$$

$$\cong P_{F_0} \exp \{-\alpha/\tau[t - t + t^2/2T]\} \tag{61}$$

$$\Rightarrow P_F(t) \cong P_{F_0} \exp \{-\alpha t^2/2T\tau\}. \tag{62}$$

Figure 11 shows the typical decay of resonator forward power during the occurrence of an arc. By fitting eq. (62) to this curve, the value of α can be found since the ring length l, the group velocity v_g, and the formative time constant T are known. The value of α was experimentally found to be

$$\alpha = 0.015. \tag{63}$$

Hence, in the steady-state, an arc struck in WR-284 waveguide filled with 25 psig of SF_6 absorbs 1.5 percent of the power which is incident upon it and reflects the remainder.

It is noted that the above method for determining the percentage of power absorbed by an arc provides greater accuracy than could be obtained by direct measurement of the power levels incident upon and reflected from the arc since the latter involves the subtraction of two nearly equal quantities.

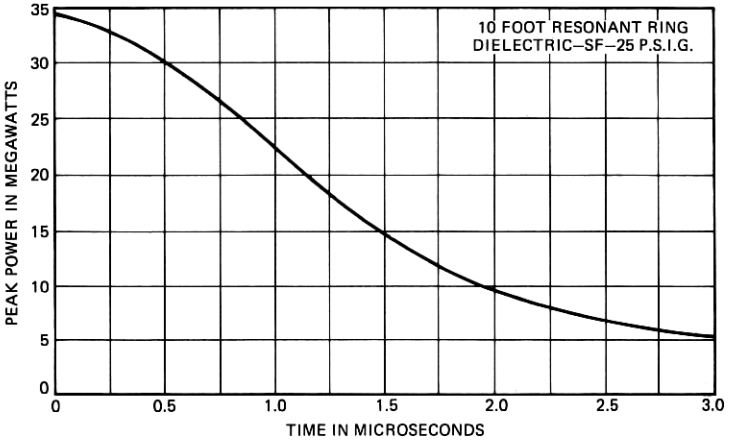

Fig. 11—Resonant ring power decay.

REFERENCES

1. MacDonald, A. D., *Microwave Breakdown in Gases*, New York: John Wiley & Sons, 1966.
2. Gould, L., and Roberts, L. W., "Breakdown of Air at Microwave Frequencies," J. App. Phy., *27*, No. 10 (October, 1956).
3. Brown, S. C., *Basic Data of Plasma Physics*, Cambridge, Mass.: Press, 1966.
4. Miller, S. J., "The Traveling Wave Resonator and High Power Microwave Testing," Microwave J., September 1960.
5. Duff, G. F. D., and Naylor, D., *Differential Equations of Applied Mathematics*, New York: John Wiley & Sons, 1966.
6. Namitokov, K. K., AD 696-315, Foreign Technology Div., Wright-Patterson AFB, Ohio, "Aggregate State, Composition and Structure of the Products 0—ETC (U)," (September 1969), FTO-MT-24-81-69.
7. Anderson, T. Reeves, A. L., Mears, W. H., and Orfeo, S. R., "The Use of Sulfur Hexafluoride in Waveguides," AIEE Conference Paper, January 1957.
8. *The Microwave Engineer's Handbook and Buyer's Guide*, Horizon House, 1965.